Dependence of energy flux from the wind to surface inertial currents on the scale of atmospheric motions

Xiaoming Zhai*

Centre for Ocean and Atmospheric Sciences, School of Environmental Sciences, University of East Anglia, Norwich, UK

Corresponding author address: Xiaoming Zhai, School of Environmental Sciences, University of East Anglia, Norwich, UK, NR4 7TJ

E-mail: xiaoming.zhai@uea.ac.uk

ABSTRACT

Atmospheric features such as translating cold fronts and small lows with horizontal scales of about 100 km are traditionally thought to be most important in exciting near-inertial motions in the ocean. However, recent studies suggest that a significant fraction of energy flux from the wind to surface inertial currents may be supplied by atmospheric systems of larger scales. Here the dependence of this energy flux on the scale of atmospheric motions is investigated using a high-resolution atmosphere reanalysis product and a slab model. It is found that mesoscale atmospheric systems with scales less than 1000 km are responsible for almost all the energy flux from the wind to near-inertial motions in mid-latitude North Atlantic and North Pacific. Transient atmospheric features with scales of $\sim$100 km contribute significantly to this wind energy flux, but they are not as dominant as traditionally thought. Owing to the nonlinear nature of the stress law, energy flux from mesoscale atmospheric systems depends critically on the existence of the background, larger-scale wind field. Finally, accounting for relative motions in the stress calculation reduces the net wind energy flux to near-inertial motions by about one-fifth. Mesoscale atmospheric systems are found to be responsible for the majority of this relative wind damping effect.

1. Introduction

Near-inertial waves generated by fluctuating winds are an important energy source for generating diapycnal mixing in both the upper and deep ocean, contributing to the cooling of the sea surface temperature (e.g Jochum et al. 2013) and the maintenance of the large-scale overturning circulation (Wunsch and Ferrari 2004). The total energy flux from the wind to surface near-inertial currents is estimated to be between 0.3 TW (1 TW = 10^{12} W) and 1.5 TW (e.g. Watanabe and Hibiya 2002; Alford 2003; Jiang et al. 2005; Furuichi et al. 2008; Rimac et al. 2013), with the spread largely explained by the different wind stress products used. Midlatitude travelling winter storms are believed to provide the bulk of this energy flux (e.g. Alford 2003; Dippe et al. 2015). The term "storm" is, however, not strictly defined and in this context it often implicitly refers to a combination of transient atmospheric phenomena including synoptic weather systems, cold/warm fronts and travelling lows that cover a wide range of spatial scales. It remains unclear what scales of atmospheric motions are responsible for the majority of energy flux to near-inertial motions in the ocean.

In the pioneering work of D'Asaro (1985), he examined wind forcing of surface inertial currents using long-term meteorological buoy data off North America, and found that near-inertial motions at his study sites are mainly excited by atmospheric features such as translating cold fronts and small lows with horizontal scales of about 100 km, with the larger-scale features making only a minor contribution. The physical explanation is that mesoscale atmospheric features in midlatitudes are typically advected by the background wind field at a speed of 10 m s^{-1}. As such, features with scales of 100 km will be advected past a given location with a time scale close to $1/f$, where f is the local inertial frequency, thereby resonantly exciting inertial currents in the surface mixed layer. Results from recent sensitivity studies of energy input to near-inertial motions by the wind (P_I) to

the resolution of wind stress forcing, on the other hand, seem to suggest that a greater fraction of P_I is provided by atmospheric systems with scales larger than that originally proposed by D'Asaro (1985). For example, in Rimac et al. (2013), although the globally-integrated P_I decreases from 1.1 TW to 0.7 TW after they spatially interpolated their wind stress forcing from the original 0.35° grid to a coarser 2.8° grid, the bulk (∼64%) of P_I remains.

It is, however, worth pointing out that the method of directly filtering wind stress used in previous sensitivity studies is appropriate for analysing the influence of high-resolution wind stress forcing on P_I, but not for assessing the role of atmospheric systems of different spatial and temporal scales in supplying P_I to the ocean owing to the nonlinear nature of the stress law (e.g. Zhai et al. 2012; Zhai 2013). For example, high-frequency wind fluctuations not only cause wind stresses to vary at high frequencies, but also contribute toward low-frequency and time-mean wind stresses and energy fluxes to the ocean (Zhai et al. 2012; Wu et al. 2016).[1] In this study, we investigate the dependence of wind energy flux to surface inertial currents on the scale of atmospheric motions using a high-resolution atmosphere reanalysis wind product and a slab model, while taking into account the nonlinear stress law.

2. Model experiment

The widely-used damped slab model originally proposed by Pollard and Millard (1970) is used in this study. The governing equation of the slab model is given by

$$\frac{dZ}{dt} + (if + r)Z = \frac{T}{H}, \tag{1}$$

where $Z = u + iv$ is the horizontal velocity, $T = (\tau_x + i\tau_y)/\rho_0$ is the surface wind stress scaled by the density of seawater, H is the surface mixed layer depth, and r is the linear damping coefficient that parameterises the decay of near-inertial motions in the mixed layer via wave radiation and

[1] see Grant and Madsen (1986) for a discussion of nonlinear stresses in the continental-shelf bottom boundary layer.

shear dissipation at the base of the mixed layer. In the slab model, Z is assumed to be mixed instantaneously over the depth of the surface mixed layer. However, a number of studies (e.g. Niiler and Paduan 1995; D'Asaro 1995; Garrett 2001; Rath et al. 2014; Kilbourne and Girton 2015) have shown that this is not always true. For example, Kilbourne and Girton (2015) found that the climatological mixed layer depths do not represent the vertical extent of wind-generated inertial currents in their float observations and argued strongly against their use in the slab model. For this reason, here we simply set $H = 50$ m and $r^{-1} = 4.5$ days (see also Zhai 2015), instead of using mixed layer depth climatologies. Following D'Asaro (1985), the solution to (1) is divided into the inertial (Z_I) and Ekman (Z_E) components, with the Ekman component given by $Z_E = T/(if+r)H$ and the inertial component given by the residual, i.e., $Z_I = Z - Z_E$. Energy flux from the wind to surface near-inertial currents is then calculated using $P_I = \rho_0 T \cdot Z_I^*$, where Z_I^* is the complex conjugate of Z_I.

The slab model is forced by the 10-m wind field taken from the hourly NCEP Climate Forecast System Reanalysis product (CFSR; Saha et al. 2010) for the period of 2001-2010. The CFSR 10-m wind is provided on a T383 grid, i.e., a horizontal resolution of $\sim 0.3^\circ$. To investigate the dependence of P_I on the scale of atmospheric motions, the original CFSR *wind* is spatially filtered using a two-dimensional mean filter to coarser grids to remove atmospheric systems with scales less than 200 km, 500 km and 1000 km, respectively, prior to the calculation of surface wind stress. The surface wind stress is then calculated from both the original and spatially-filtered CFSR winds based on the bulk formula (Large et al. 1994). To highlight the effect of the nonlinear stress law, surface wind *stresses* calculated from the original CFSR winds are also spatially filtered to the same 200 km, 500 km and 1000 km grids, as often done in previous studies (e.g. Rimac et al. 2013).

3. Results

a. Scale dependence of P_I

Figure 1a shows energy flux from the wind to surface near-inertial motions, P_I, in the midlatitude North Atlantic ([30°-70°N, 82°W-0°]) averaged over the decade of 2001-2010. The spatial pattern of P_I is characterised by large positive values concentrated in the storm track region and small/moderate values elsewhere, in general agreement with previous studies (e.g. Alford 2003; Furuichi et al. 2008; Rimac et al. 2013; Dippe et al. 2015). To the south of the Gulf Stream, there are tracks of high values of P_I associated with moving hurricanes. Removing wind variability with scales less than 200 km in the stress calculation reduces the domain-averaged P_I by about 30% from 1.17 mW m^{-2} to 0.82 mW m^{-2} (Fig. 1b). Interestingly, the bulk of P_I remains in the absence of atmospheric motions with scales of $\sim$100 km that are traditionally thought to be most important and efficient in exciting near-inertial motions in the ocean (e.g. D'Asaro 1985). Further removing atmospheric motions with scales less than 500 km in the stress calculation reduces the domain-averaged P_I by about 70%, and removing atmospheric motions with scales less than 1000 km gets rid of almost all the P_I (over 92%; Figs. 1c and d). These results show that wind forcing of near-inertial motions in the ocean results from a combination of mesoscale atmospheric systems with scales less than 1000 km that presumably propagate at a range of speeds, rather than being dominated by features with scales of $\sim$100 km propagating at a typical speed of 10 m s^{-1} as traditionally thought. A similar reduction in P_I is also found in the midlatitude North Pacific ([20°-60°N, 125°E-120°W]) when mesoscale atmospheric features are excluded in the stress calculation (Fig. 2; see also Table 1), although the magnitude of P_I in the North Pacific is generally higher than that in the North Atlantic.

Since the slab model is linear, the reduction of P_I found in this study has to be a direct result of the decrease in the magnitude of inertial wind stress forcing when mesoscale wind fields are removed in the stress calculation. Figure 3 shows the zonally-averaged zonal wind stress spectra at 50°N and 35°N in the North Atlantic. Removing mesoscale wind variability is found to reduce the power of wind stress at all frequencies at both latitudes (Figs. 3a and d). In particular, the magnitude of inertial wind stress forcing decreases by about 32%, 72% and 93%, respectively, when atmospheric motions with scales less than 200 km, 500 km and 1000 km are removed prior to stress calculation. These percentage decreases in the magnitude of inertial wind stress forcing are indeed very close to the percentage reductions in P_I, as one would expect. Similar results are also found at other latitudes in the North Atlantic as well as in the North Pacific (not shown).

Associated with the seasonal variability of atmospheric storm tracks, P_I exhibits a pronounced seasonal cycle in both the North Atlantic and North Pacific: P_I in winter months is over an order of magnitude greater than that in summer months (Fig. 4). The reduction in P_I when mesoscale atmospheric features are removed in the stress calculation follows the same seasonal cycle with the most significant reduction occurring during winter while almost no reduction during summer. In other words, seasonal variations in the strength of mesoscale atmospheric phenomena strongly enhance the seasonal cycle of P_I. The percentage reduction of P_I, on the other hand, shows much less seasonal variations: 25-40%, 60-80% and 90-95% in the absence of atmospheric motions with scales less than 200 km, 500 km and 1000 km, respectively (Figs. 4c and d). There is little difference between the North Atlantic and North Pacific in terms of percentage reductions in P_I, suggesting that the scale dependence of P_I found in this study may apply to other ocean basins as well.

b. Nonlinear stress law

In this subsection, we seek to address two questions related to the nonlinear nature of the stress law: (1) is there a noticeable difference between methods of averaging *wind* and averaging *stress* in assessing the contribution of mesoscale atmospheric phenomena to P_I? and (2) do the larger-scale atmospheric motions matter?

Figure 5 shows P_I in the midlatitude North Atlantic and North Pacific averaged over the period of 2001-2010 when surface wind stresses calculated from the original CFSR winds are spatially filtered to remove wind stress variability with scales less than 200 km, 500 km and 1000 km, as is often done in previous sensitivity studies (e.g. Rimac et al. 2013). Although the spatial patterns remain quite similar, there are some quantitative differences in P_I between averaging *stress* (Fig. 5) and averaging *wind* (Figs. 1 and 2). Owing to the nonlinear stress law, mesoscale winds contribute to wind stresses not only at mesoscales but also at larger scales (e.g. Zhai et al. 2012). As a result, the reduction of P_I is greater (roughly by 10%) when the winds, rather than wind stresses, are spatially filtered. For example, about 74%, 35% and 10% of P_I in the North Pacific remains when the CFSR 10-m winds with scales less than 200 km, 500 km and 1000 km are removed prior to the calculation of surface wind stress, comparing to 81%, 46% and 18% remaining when CFSR wind stresses at the same scales are removed (Table 1). This quantitative difference in the reduction of P_I between averaging stress and averaging wind is consistent with the more tightly-grouped curves of wind stress spectra in Figs. 3b and e than in Figs. 3a and d; directly filtering wind stresses leads to a smaller decrease in the power of wind stress at all frequencies than filtering the wind field prior to stress calculation (by $\sim$10% at inertial frequencies).

Another interesting consequence of the nonlinear stress law is that the effect of wind fluctuations on wind stress depends strongly on the presence of the large-scale background winds (Zhai

2013). For example, the mean wind stress vanishes in regions of zero mean winds, regardless of the strength of wind fluctuations there, owing to the modulus sign in the stress formula. Figure 6 shows P_I in the midlatitude North Atlantic and North Pacific when only mesoscale atmospheric motions with scales less than 200 km, 500 km and 1000 km are included in the stress calculation. In the absence of atmospheric motions with scales greater than 200 km, 500 km and 1000 km, merely 0.2%, 2% and 10%, respectively, of P_I remains in each ocean basin, as a result of the orders of magnitude decrease in the strength of inertial wind stress forcing (Figs. 3c and f). This striking result demonstrates that although mesoscale atmospheric systems play a fundamental role in supplying P_I to the ocean, the role they play depends critically on the existence of the background, larger-scale wind field owing to the nonlinear nature of the stress law. Studies on the variability and trend of P_I (e.g. Alford 2003; Dippe et al. 2015; Zhai 2015) therefore need to take into account not only changes of mesoscale atmospheric systems but also the background large-scale wind field.

A recent study (Rath et al. 2013) found that including ocean surface velocity in the wind stress calculation led to a noticeable reduction of P_I in the Southern Ocean owing to the relative wind damping effect, an effect not accounted for in previous estimates of P_I (e.g. Alford 2003; Jiang et al. 2005; Furuichi et al. 2008; Rimac et al. 2013). The relative wind damping effect arises because accounting for relative motions in the stress calculation systematically reduces the positive wind work when the wind and ocean surface current are aligned and enhances the negative wind work when they oppose each other (Zhai et al. 2012). Here we investigate this relative wind damping effect on P_I in the North Atlantic and North Pacific as well as its dependence on spatial scales. Figure 7 shows that accounting for relative motions in the stress calculation leads to a wide-spread reduction in P_I. The reduction of P_I is most significant in the storm track regions where the winds are particularly strong, since the relative wind damping effect is proportional to

the speed of 10-m winds (Duhaut and Straub 2006; Zhai et al. 2012; Rath et al. 2013). Averaged over the midlatitude North Atlantic and North Pacific, P_I decreases by about 20% in both ocean basins, similar to what Rath et al. (2013) found in a model of the Southern Ocean. Furthermore, the relative wind damping effect of P_I shows a pronounced seasonal cycle, with large damping effect in winter months and almost no damping in summer months (Figs. 4a and b). As such, accounting for relative motions in the stress calculation acts to reduce the amplitude of the seasonal cycle of P_I. Finally, the effect of relative wind damping of P_I depends strongly on the presence of mesoscale atmospheric features. Removing atmospheric features with scales less than 200 km, 500 km and 1000 km in the stress calculation reduces the damping effect by about 32%, 74% and 95%, respectively.

4. Concluding remarks

The dependence of energy flux from the wind to surface inertial currents on the scale of atmospheric motions has been investigated in this study using a high-resolution atmospheric reanalysis product and a slab model. Our main findings are as follows:

- Mesoscale atmospheric systems with horizontal scales less than 1000 km are responsible for almost all the P_I to the ocean.

- Transient atmospheric features with scales of $\sim$100 km contribute significantly (about 25-30%) to P_I, but they are not as dominant as traditionally thought.

- Owing to the nonlinear nature of the stress law, P_I from mesoscale atmospheric systems depends critically on the existence of the background, larger-scale wind field.

- Accounting for relative motions in the stress calculation reduces the net P_I by about one-fifth. Mesoscale atmospheric systems are found to be responsible for the majority of this energy flux reduction.

It is well known (e.g. Gill 1984; D'Asaro 1989) that the rate at which the wind-induced near-inertial energy radiates away from the mixed layer is inversely proportional to the scale of atmospheric forcing squared, the rate being greatest for the smallest scales. Therefore, whether P_I is primarily supplied by transient atmospheric features with horizontal scales of $\sim$100 km or by those of larger scales may have important consequences for the efficiency of near-inertial energy flux into the ocean interior, with implications for the interior near-inertial mixing. In this study, the bulk of P_I is found to be supplied by atmospheric motions with scales greater than 200 km, suggesting a lower efficiency of near-inertial energy flux into the ocean interior than it would have been if P_I were supplied by transient atmospheric features with scales of $\sim$100 km as traditionally thought.

On the other hand, the remarkable coincidence between atmospheric and oceanic storm tracks means that regions of large P_I are also regions of enhanced mesoscale variability in the ocean (Zhai et al. 2005). A number of studies (e.g. Weller 1982; Kunze 1985; Zhai et al. 2005; Danioux et al. 2008) have shown that the horizontal scales of near-inertial motions in the surface mixed layer in strongly eddying regions are often set by the oceanic eddy field, rendering the rate at which near-inertial energy radiates downward into the interior much less sensitive to the scales of atmospheric forcing. Future research is required to unravel the relative importance of atmospheric forcing and oceanic eddy field in setting the scales of near-inertial motions in the ocean.

Finally, our results imply that wind forcing of near-inertial motions in the ocean is a result of mesoscale atmospheric features with scales less than 1000 km propagating at a range of speeds

over a given location, rather than being dominated by features with scales of $\sim$100 km propagating at a typical speed of 10 m s^{-1}. Efforts are currently underway to identify and categorise (e.g., type, size and translational speed) transient mesoscale atmospheric phenomena that constitute the major near-inertial wind forcing of the ocean by applying automatic tracking algorithms (e.g. Hodges 1994; Blender and Schubert 2000) to high-resolution atmospheric reanalysis products.

Acknowledgments. Financial support from the School of Environmental Sciences, University of East Anglia, is gratefully acknowledged. I thank two anonymous reviewers for their constructive comments that led to a much improved manuscript. The research presented in this paper was carried out on the High Performance Computing Cluster supported by the Research and Specialist Computing Support service at the University of East Anglia.

References

Alford, M. H., 2003: Improved global maps and 54-years history of wind-work on ocean inertial motions. *Geophys. Res. Lett.*, **30(8)**, 1424, doi:10.1029/2002GL016614.

Blender, R., and M. Schubert, 2000: Cyclone tracking in different spatial and temporal resolutions. *Mon. Wea. Rev.*, **128**, 377–384.

Danioux, E., P. Klein, and P. Riviére, 2008: Propagation of wind energy into the deep ocean through a fully turbulent mesoscale eddy field. *J. Phys. Oceanogr.*, **38**, 2224–2241.

D'Asaro, E. A., 1985: The energy flux from the wind to near-inertial motions in the surface mixed layer. *J. Phys. Oceanogr.*, **15**, 1043–1059.

D'Asaro, E. A., 1989: The decay of wind-forced mixed layer inertial oscillations due to the β effect. *J. Geophys. Res.*, **94**, 2045–2056.

D'Asaro, E. A., 1995: Upper-ocean inertial currents forced by a strong storm. Part II: Modelling. *J. Phys. Oceanogr.*, **25**, 2937–2952.

Dippe, T., X. Zhai, R. J. Greatbatch, and W. Rath, 2015: Interannual variability of wind power input to near-inertial motions in the north atlantic. *Ocean Dyn.*, **65**, 859–875.

Duhaut, T. H., and D. N. Straub, 2006: Wind stress dependence on ocean surface velocity: Implications for mechanical energy input to ocean circulation. *J. Phys. Oceanogr.*, **36**, 202–211.

Furuichi, N., T. Hibiya, and Y. Niwa, 2008: Model-predicted distribution of wind-induced internal wave energy in the world's oceans. *J. Geophys. Res.*, **113**, 09034, doi:10.1029/2008JC004768.

Garrett, C., 2001: What is the "Near-Inertial" band and why is it different from the rest of the internal wave spectrum. *J. Phys. Oceanogr.*, **31**, 962–971.

Gill, A. E., 1984: On the behavior of internal waves in the wakes of storms. *J. Phys. Oceanogr.*, **14**, 1129–1151.

Grant, W. D., and O. S. Madsen, 1986: The continental-shelf bottom boundary layer. *Ann. Rev. Fluid Mech.*, **18**, 265–305.

Hodges, K. I., 1994: A general method for tracking analysis and its application to meteorological data. *Mon. Wea. Rev.*, **122**, 2573–2586.

Jiang, J., Y. Lu, and W. Perrie, 2005: Estimating the energy flux from the wind to ocean inertial motions: the sensitivity to surface wind fields. *Geophys. Res. Lett.*, **32**, L15 610.

Jochum, M., B. P. Briegleb, G. Danabasoglu, W. G. Large, N. J. Norton, S. R. Jayne, and F. O. Bryan, 2013: The impact of oceanic near-inertial waves on climate. *J. Clim.*, **26**, 2833–2844.

Kilbourne, B. F., and J. B. Girton, 2015: Quantifying high-frequency wind energy flux into near-inertial motions in the southeast pacific. *J. Phys. Oceanogr.*, **45**, 369–386.

Kunze, E., 1985: Near-inertial propagation in geostrophic shear. *J. Phys. Oceanogr.*, **15**, 544–565.

Large, W. G., J. C. McWilliams, and S. C. Doney, 1994: Oceanic vertical mixing: A review and a model with a nonlocal boundary layer parmeterization. *Rev. Geophys.*, **32**, 363–403.

Niiler, P., and J. D. Paduan, 1995: Wind-driven motions in the northeast Pacific as measured by Lagrangian drifters. *J. Phys. Oceanogr.*, **25**, 2819–2830.

Pollard, R. T., and R. C. J. Millard, 1970: Comparison between observed and simulated wind-generated inertial oscillations. *Deep-Sea Res.*, **17**, 153–175.

Rath, W., R. J. Greatbatch, and X. Zhai, 2013: Reduction of near-inertial energy through the dependence of wind stress on the ocean-surface velocity. *J. Geophys. Res.*, **118**, 2761–2773.

Rath, W., R. J. Greatbatch, and X. Zhai, 2014: On the spatial and temporal distribution of near-inertial energy in the Southern Ocean. *J. Geophys. Res.*, **119**, 359–376.

Rimac, A., J. S. von Storch, C. Eden, and H. Haak, 2013: The influence of high-resolution wind stress field on the power input to near-inertial motions in the ocean. *Geophys. Res. Lett.*, **40**, 4882–4886.

Saha, S., and Coauthors, 2010: The NCEP climate forecast system reanalysis. *Bull. Amer. Meteor. Soc.*, **91**, 1015–1057.

Watanabe, M., and T. Hibiya, 2002: Global estimates of the wind-induced energy flux to inertial motions in the surface mixed layer. *Geophys. Res. Lett.*, **29**, 1239, doi:10.1029/2001GL014422.

Weller, R. A., 1982: The relationship of near-inertial motions observed in the mixed layer during the JASIN(1978) experiment to the local wind stress and to the quasi-geostrophic flow field. *J. Phys. Oceanogr.*, **12**, 1122–1136.

Wu, Y., X. Zhai, and Z. Wang, 2016: Impact of synoptic atmospheric forcing on the mean ocean circulation. *J. Clim.*, **29**, 5709–5724.

Wunsch, C., and R. Ferrari, 2004: Vertical mixing, energy, and the general circulation of the oceans. *Annu. Rev. Fluid Mech.*, **36**, 281–314.

Zhai, X., 2013: On the wind mechanical forcing of the ocean general circulation. *J. Geophys. Res.*, **118**, 6561–6577, doi:10.1002/2013JC009086.

Zhai, X., 2015: Latitudinal dependence of wind-induced near-inertial energy. *J. Phys. Oceanogr.*, **45**, 3025–3032.

Zhai, X., R. J. Greatbatch, and J. Zhao, 2005: Enhanced vertical propagation of storm-induced near-inertial energy in an eddying ocean channel model. *Geophys. Res. Lett.*, **32**, 18602, doi: 10.1029/2005GL023643.

Zhai, X., H. L. Johnson, D. P. Marshall, and C. Wunsch, 2012: On the wind power input to the ocean general circulation. *J. Phys. Oceanogr.*, **42**, 1357–1365, doi:10.1175/JPO-D-12-09.1.

LIST OF TABLES

TABLE 1. Effect of spatially filtering wind and wind stress on the domain-averaged energy flux from the wind to surface near-inertial motions in the midlatitude North Atlantic (mid-NA; [30°-70°N, 82°W-0°]) and midlatitude North Pacific (mid-NP; [20°-60°N, 125°E-120°W]).

	removing scales $<$ 200 km	removing scales $<$ 500 km	removing scales $<$ 1000 km
P_I remaining in mid-NA after spatially-filtering wind	70%	30%	8%
P_I remaining in mid-NA after spatially-filtering wind stress	78%	40%	15%
P_I remaining in mid-NP after spatially-filtering wind	73%	34%	10%
P_I remaining in mid-NP after spatially-filtering wind stress	81%	46%	18%

LIST OF FIGURES

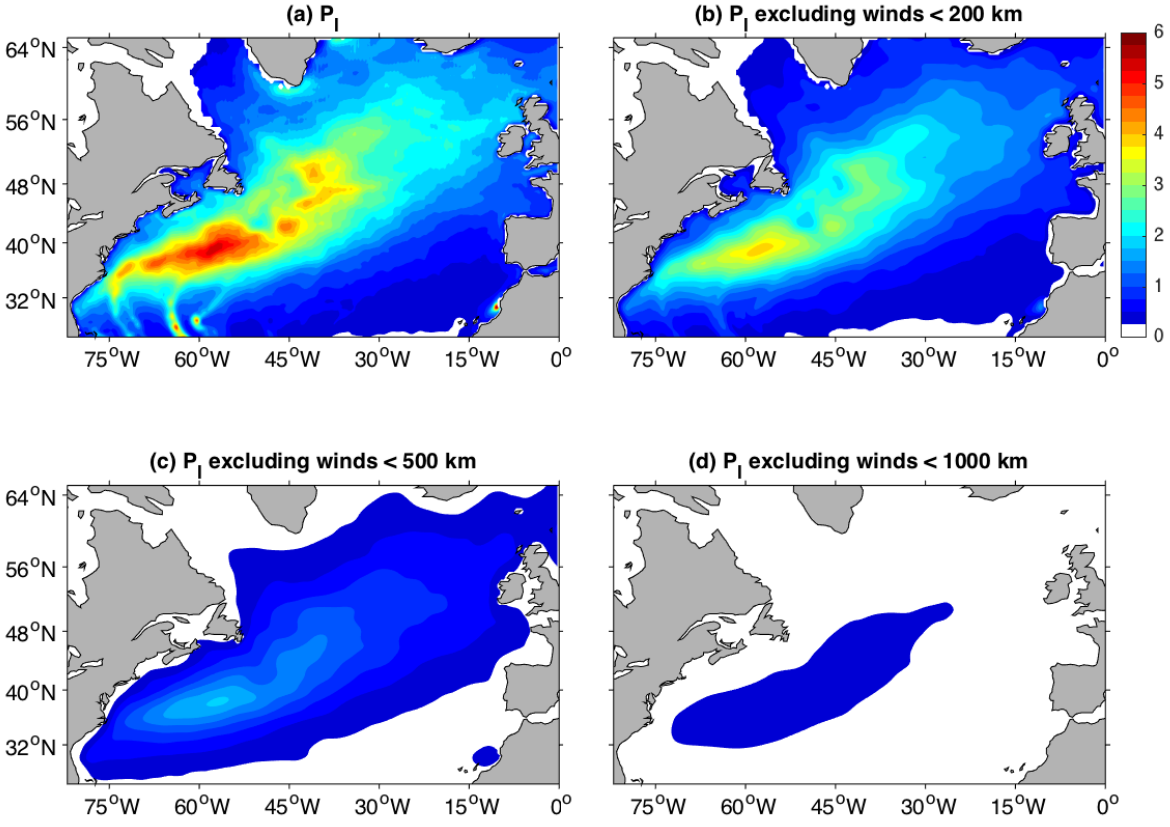

FIG. 1. Energy flux (mW m^{-2}) from the wind to near-inertial motions in the midlatitude North Atlantic averaged over the period of 2001-2010 when (a) the original CFSR winds, and CFSR winds excluding wind variability with scales less than (b) 200 km, (c) 500 km and (d) 1000 km, are used in the stress calculation.

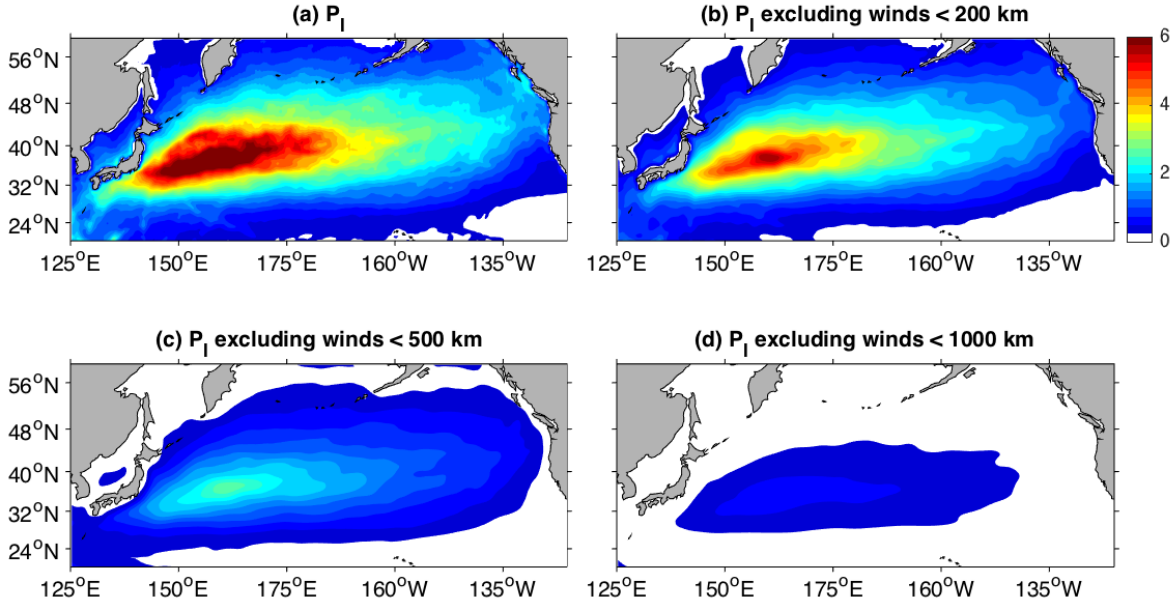

FIG. 2. Same as Fig. 1 but for the midlatitude North Pacific.

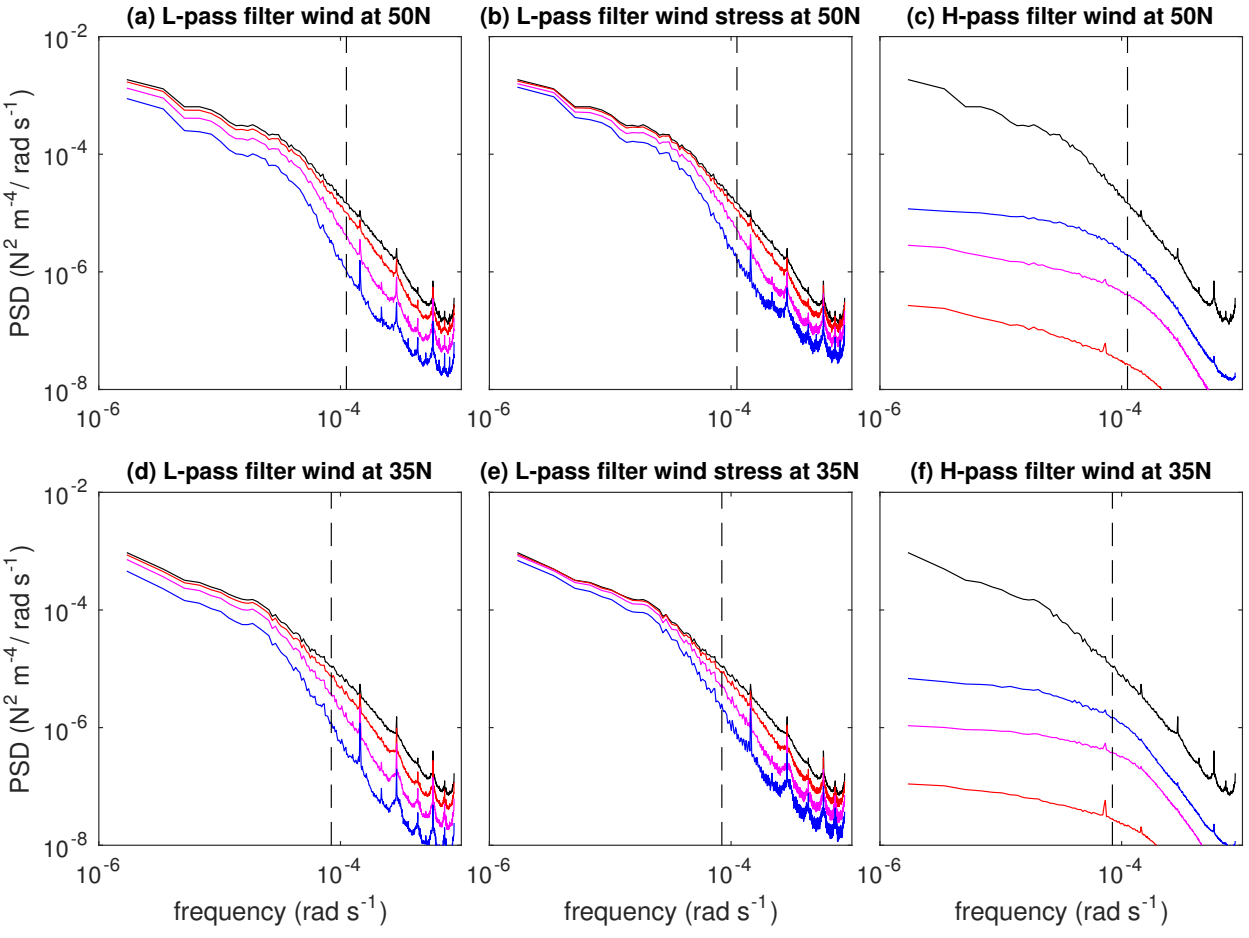

FIG. 3. Zonally-averaged zonal wind stress spectra at 50°N in the North Atlantic when (a) low-pass spatially-filtering the wind field prior to stress calculation, (b) directly low-pass filtering wind stresses and (c) high-pass filtering the wind field prior to stress calculation. The solid black curve in each panel represents the spectra of zonal wind stresses calculated from the original CFSR wind field, and the red, magenta and blue curves represent respectively the spectra of wind stresses that are either directly filtered with cutoff scales of 200 km, 500 km and 1000 km or calculated from the wind fields that are low-pass or high-pass filtered at those scales. The vertical dashed black line marks the local inertial frequency. (d)-(f) are the same as (a)-(c), but for the zonally-averaged zonal wind stress spectra at 35°N in the North Atlantic. The subharmonic spectra peaks are likely to be an artefact of the reanalysis product.

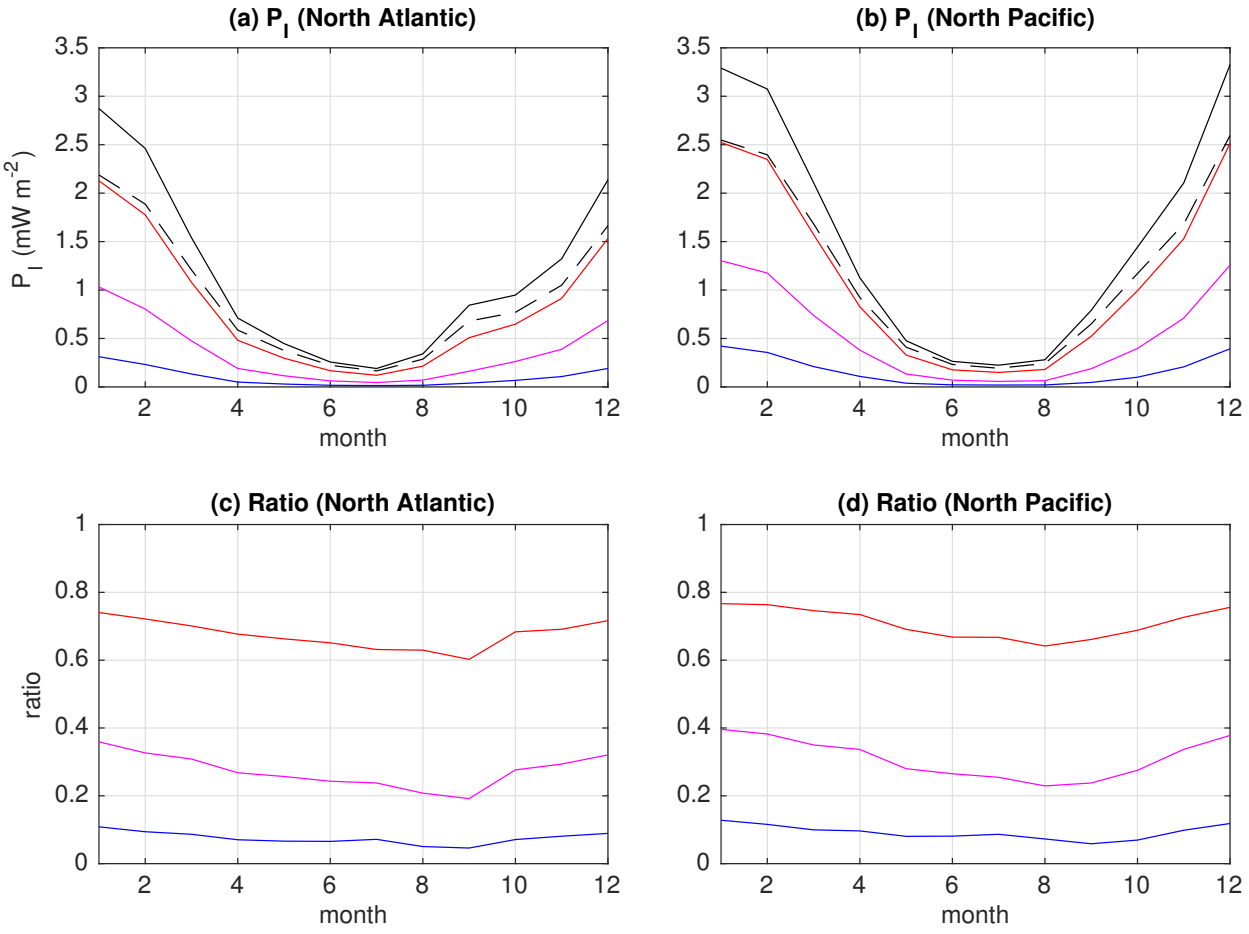

FIG. 4. Seasonal cycles of P_I in the midlatitude (a) North Atlantic and (b) North Pacific when the original CFSR winds (black), and CFSR winds excluding wind variability with scales less than 200 km (red), 500 km (magenta) and 1000 km (blue), are used in the stress calculation. The ratios of red, magenta and blue curves over the black curve in (a) and (b) are shown in the same colours in (c) and (d) respectively. The dashed lines in (a) and (b) are P_I in the midlatitude North Atlantic and North Pacific when the relative wind effect is accounted for in the stress calculation.

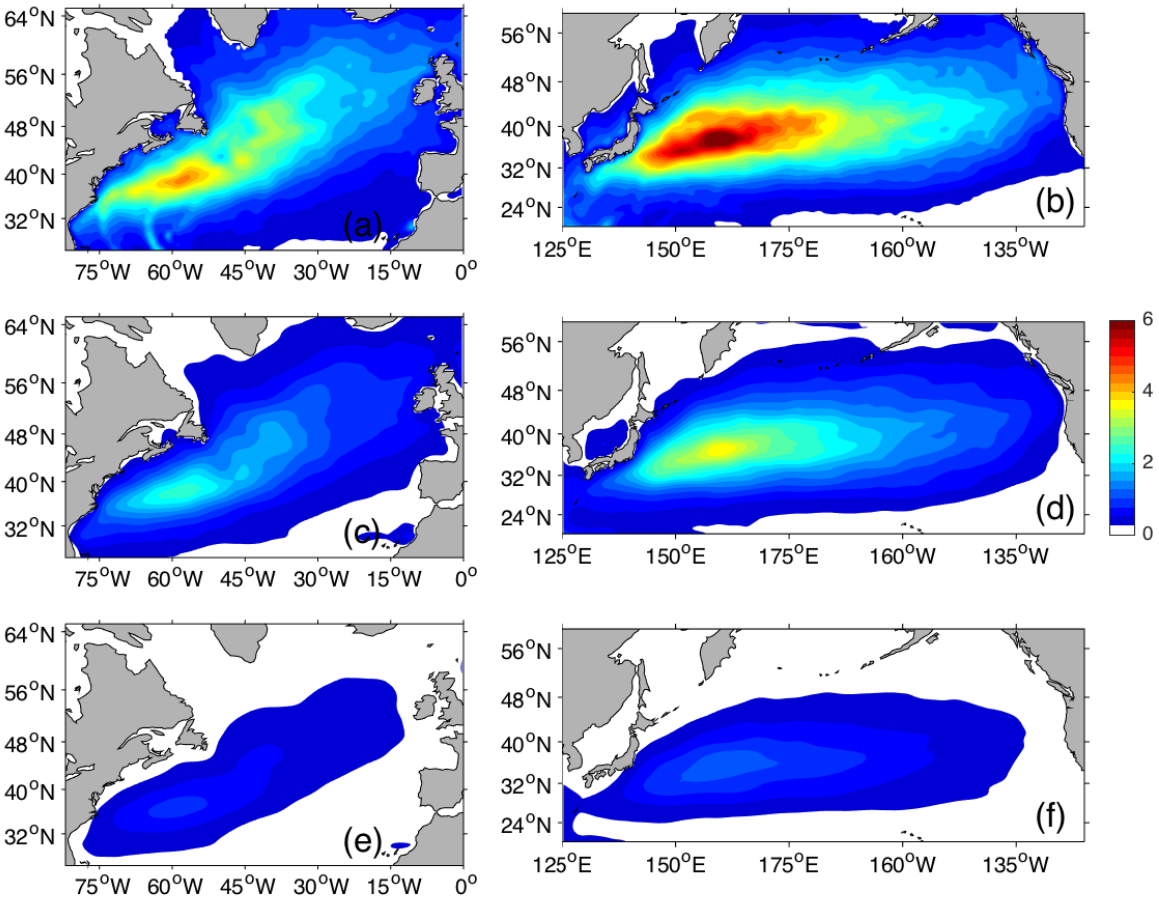

363 FIG. 5. (a), (c) and (e) are P_I (mW m^{-2}) in the midlatitude North Atlantic when wind stresses calculated from
364 the original CFSR winds are spatially-filtered to remove wind stress variability with scales less than 200 km,
365 500 km and 1000 km, respectively. (b), (d) and (f) are the same as (a), (c) and (e) but for the North Pacific.

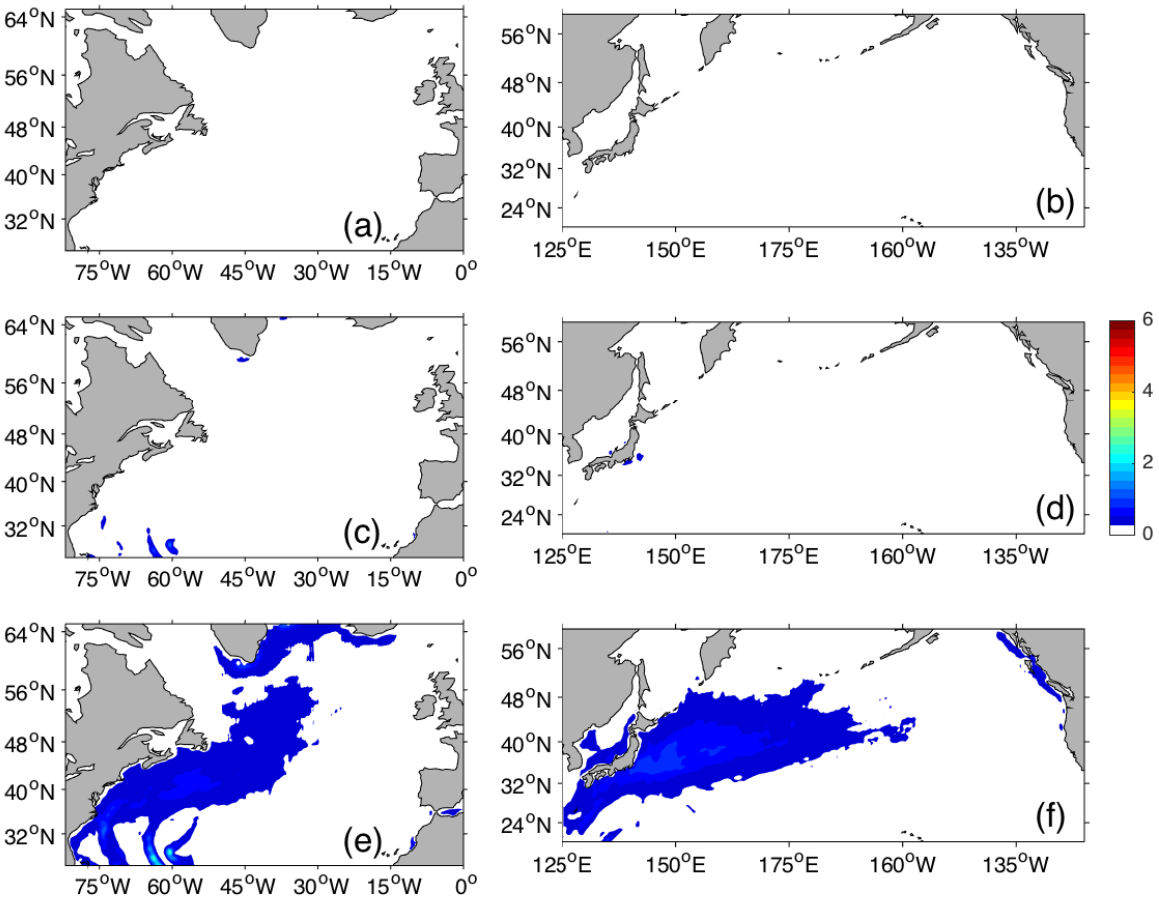

366 FIG. 6. (a), (c) and (e) are P_I (mW m^{-2}) in the midlatitude North Atlantic when only atmospheric motions
367 with scales less than 200 km, 500 km and 1000 km are included in the stress calculation. (b), (d) and (f) are the
368 same as (a), (c) and (e) but for the North Pacific.

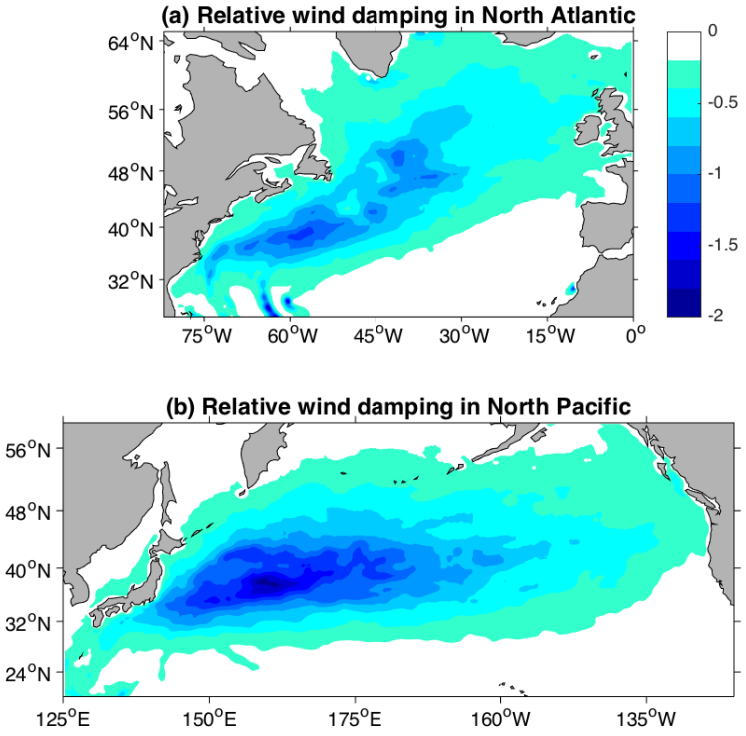

369 FIG. 7. The relative wind damping of P_I (mW m^{-2}) averaged over the period of 2001-2010 in the midlatitude
370 (a) North Atlantic and (b) North Pacific.